Journal of Hydrology 585 (2020) 124759

Contents lists available at ScienceDirect

Journal of Hydrology

journal homepage: www.elsevier.com/locate/jhydrol

Research papers

On the complexities of sediment load modeling using integrative machine learning: Application of the great river of Loíza in Puerto Rico

Mohammad Zounemat-Kermani[a,*], Amin Mahdavi-Meymand[b], Meysam Alizamir[c], S. Adarsh[d], Zaher Mundher Yaseen[e,*]

[a] Water Engineering Department, Shahid Bahonar University of Kerman, Kerman, Iran
[b] Water Engineering Department, Shahid Bahonar University of Kerman, Kerman, Iran
[c] Department of Civil Engineering, Hamedan Branch, Islamic Azad University, Hamedan, Iran
[d] Department of Civil Engineering, TKM College of Engineering Kollam, Kollam, India
[e] Institute of Research and Development, Duy Tan University, Da Nang 550000, Viet Nam

ARTICLE INFO

This manuscript was handled by G. Syme, Editor-in-Chief, with the assistance of Li He, Associate Editor

Keywords:
Heuristic algorithms
Soft computing
Hydrology
Bed load
River engineering

ABSTRACT

Sediment transportation in water bodies may cause many problems for the water resources projects and damage the environment. Hence, modeling sediment load components, including suspended sediment load (SSL) and bedload (BL) in rivers is of prime importance. Effective modeling of SSL and BL remains a challenging task due to their complex hydrological process. On this account, this study aims to appraise the potential of conventional machine learning (ML) models including adaptive neuro-fuzzy inference system (ANFIS), support vector regression (SVR), and their integrative version with nature optimization algorithm called genetic algorithm (GA-ANFIS and GA-SVR) for SSL and BL prediction. Two traditional models are developed for modeling verification including the sediment rating curve (SRC) and multiple linear regression (MLR). The modeling results are assessed using four statistical measures (e.g., root mean square error (*RMSE*), mean absolute error (*MAE*), Nash–Sutcliffe Efficiency (*NSE*), and coefficient of determination (R^2)), diagnostic analysis (scatter plots and Taylor diagram), and evaluation of the dependence of the state of the river flow-sediment system (hysteresis analysis). Based on the attained predictability performance, the integrative ML models reveal a superior prediction capacity in comparison with the standalone ANFIS, SVR, and the traditional models. In quantitative evaluation, the proposed integrative ML models indicate a remarkable prediction enhancement approximately 44% mean magnitude based on the *MAE* metric against the SRC traditional model for both the SSL and BL predicted values. Overall, the current investigation evidences the potential of the nature-inspired algorithm as a hyper-parameter optimizer for ML models that produce a reliable and robust predictive model for sediment concentration quantification.

1. Introduction

1.1. Background and motivation

In river engineering, sediment load is defined as the total amount of sediment output transported by rivers and streams from a watershed. Accurate estimation of sediment load is crucial to river engineering and management, including stable channel design, river restoration, as well as issues related to the water quality of the river. The changes in sediment load and transportation in rivers, which may get influenced by spatial and temporal factors, can follow an extreme nonlinear process (Fan and Yao, 2008; Kuai and Tsai, 2012; Sadeghi and Mostafazadeh, 2016).

At the larger time scales, the climatic and anthropogenic factors and all the events within the season will be influencing the sediment load patterns. The spatial and temporal changes in the watershed characteristics like vegetation cover and soil moisture condition can influence the transport processes of sediment load (Lyn, 1987). Henceforth, given the complex and nonlinear behavior of the sediment transport process, which is influenced by different watershed hydrographic and hydraulic flow factors, it is not easy to construct an accurate sediment estimation tool (Kisi and Yaseen, 2019a; Kiyoumars Roushangar and Shahnazi, 2019).

The sediment loads of a watershed can be divided into three groups including bedload (BL), suspended sediment load (SSL), and wash load. Fine sediments fall within SSL, and may be carried long distances before

* Corresponding authors.
E-mail addresses: zounemat@uk.ac.ir (M. Zounemat-Kermani), zahermundheryaseen@duytan.edu.vn (Z.M. Yaseen).

https://doi.org/10.1016/j.jhydrol.2020.124759
Received 3 December 2019; Received in revised form 14 February 2020; Accepted 23 February 2020
Available online 25 February 2020

deposition, even under the base and low-flow conditions (Salih et al., 2019a). On the other hand, BL is generally composed of coarse-grained sediments that comprise a significant volume of sediment at higher discharges and floods. Given the varying sedimentation behaviors in SSL and BL states, as well as the complexity of the transitional sedimentation phenomena in rivers, it is necessary to use models capable of capturing complex processes (Haddadchi et al., 2013b; Zounemat-Kermani et al., 2016). The wash load consists of very fine and cohesive sediments (Haddadchi et al., 2013a). Since there was no available measured data for the wash load in this study, we have excluded this type of sediment transportation and have focused on BL and SSL for the sediment load prediction (Tao et al., 2019).

The accuracy of the sediment prediction models depends on several temporal and spatial factors, including the measurement scale of data (such as daily, weekly, or monthly), data length, input variables selected, etc. In addition, the sediment load in rivers results from weathering, land sliding, and glacial and fluvial erosion (Baniya et al., 2019). The highly diverse composition of sediment load and bedload make the sediment transport modeling a complex problem and the input selection procedure is a crucial step in this exercise. The area of the catchment, land cover, slope, and topography of the catchment, rainfall (intensity and volume), temperature, soil characteristics, etc. are some of the key factors influencing SSL and BL from the basin. Traditional flow-based methods, such as the sediment rating curve (SRC), do not have a great ability to estimate sediment transportation due to reliance on sediment loads versus discharge (Rajaee et al., 2011).

1.2. Literature review: Machine learning and sediment modeling

Many studies reported that the use of lagged values of river discharge, suspended sediment, and precipitation is sufficient for the prediction of SSL (Kakaei Lafdani et al., 2013; Adnan et al., 2019; Salih et al., 2019b). The accurate prediction of BL is more difficult than SSL and predictor set for modeling BL. Researchers in the past considered different combinations of input parameters for improving the accuracy of BL predictions. The input data for BL predictions can be prepared considering hydraulic characteristics alone or using hydraulic and sediment properties, but often constrained by the availability of datasets. To cope with this setback, different researches included hydraulic properties like discharge, velocity, channel properties like Manning's roughness, particle size, channel dimensions, etc. for the prediction of bedload (Azamathulla et al., 2009; Chang et al., 2012). Haddadchi et al. (2012) investigated the suitability of different bedload transport formulae considering the field datasets Node River from north-eastern Iran, accounting several universal bedload predictors. (Haddadchi et al., 2013b) made a comprehensive investigation on the suitability of twelve popular predictive bedload transport equations against bedload and bed material grain size as inputs. They found that the sediment transport equations are sensitive to these input parameters.

Bedload transport has a dynamic nature in gravel-bed rivers, and the complexity of the phenomenon induces uncertainties in predictions (Riahi-Madvar and Seifi, 2018). Kitsikoudis et al. (2014) reported that the combination of hydraulic parameters involving unit stream power, stream power, and shear stress depicts the prediction of BL transport in the best way. Pektas and Dogan, (2015) attempted to include suspended sediment load data along with the hydraulic parameters for the prediction of BL and reported an improvement in the performance of BL prediction models. They reported that the presence of a high value of sediment load leads to poor performance, and its exclusion improved the performance. Roushangar and Shahnazi (2019) considered two scenarios for the model inputs of sediment transport based on 1) only hydraulic characteristics, and 2) both hydraulic and sediment factors. They reported an improvement in sediment load prediction on considering the second scenario.

Given the emergence of machine learning (ML) models in recent decades and their superiority in simulating many hydrological issues compared to experimental methods, these models have been used increasingly for the estimation of sediment transport (Sharghi et al., 2019b; Yilmaz et al., 2018; Zounemat-Kermani, 2017). In recent years, several successful applications of machine learning (ML) in simulating sediment transport have been reported given the hydraulic data, such as river flow discharge (Adnan et al., 2019; Afan et al., 2015; Baniya et al., 2019).

Parallel to the usage of standard ML models, some researchers tried to get the advantages of integrative machine learning models in simulating sediment load in rivers. Memarian et al. (2013) employed an integrative ML model based on the combination of multi-layer perceptron (MLP) neural network and genetic algorithm (GA) for sediment load simulation in a tropical watershed. It was reported that the integrative GA-MLP model presented a reliable performance for sediment load modeling. Sahraei et al. (2017) coupled particle swarm optimization (PSO) algorithm to calibrate the regularization and kernel parameters of least square support vector regression (LSSVR) as an alternative integrative method for estimating SSL in channels. The findings of the study proved the superiority of the integrative ML model in SSL estimation in comparison to traditional ML models. Yadav et al. (2018) applied a genetic algorithm (GA) for developing two types of integrative models such as artificial neural networks (ANN) and support vector machines (SVM) for sediment load prediction. In comparison to the standard version of the applied ML models, the results showed that integrative ML models are better candidates for simulation of the SSL prediction. Roushangar and Shahnazi (2019) challenged the potential of an integrative PSO-WKELM model (a wavelet kernel extreme learning machine coupled with the particle swarm optimization algorithm) versus standard ML model in predicting BL in rivers. The findings of the study confirmed the higher predictive potential of the PSO-WKELM integrative ML model in comparison with SVM as a standard ML model.

Studying published works in the use of ML methods in sediment modeling implies that the majority of researches focused on using ML models in simulating suspended sediment load (SSL) compared to bedload (BL) (Choubin et al., 2018; Khosravi et al., 2018; Khan et al., 2019; Kumar et al., 2019). Due to a large number of published pertinent studies using ML models in SSL and BL modeling, reporting and covering them requires an ample space, which is beyond the aim of this paper. However, to gain a general concept, a concise summary of the most updated research published is presented in Table 1.

As shown in Table 1, the majority of studies on sediment transport modeling in rivers have focused on SSL simulation. Also, no comprehensive study similar to the present research was found to investigate the simultaneous deposition of sediment transport in SSL and BL based on the flow data.

1.3. Objectives and contribution of the study

Despite the contributions of various traditional ML studies in sediment load modeling, many researchers have emphasized the necessity of integrating *meta*-heuristic algorithms with standard ML models to obtain better results in modeling complex phenomena (Rajaee et al., 2011; Zounemat-Kermani, 2017; Kisi et al., 2019; Zounemat-Kermani et al., 2019). Therefore, this study aims to evaluate the performance of traditional methods (SRC & MLR), standard ML methods (ANFIS & SVR), and integrative ML and nature-inspired methods (GA-ANFIS & GA-SVR) in predicting sediment load including SSL and BL. For this purpose, daily long-term sediment transport data along the flow discharge of the Grande de Loíza River in Puerto Rico are used. Comparing and appraising the performance of different traditional statistical methods as well as standard and integrative ML models in simulating both SSL and BL is the main novelty of this paper. Besides, exploring previous hydrological studies also shows that evaluating ANFIS and SVR methods, as integrative models, is only limited to scour prediction around bridge piers (Sreedhara et al., 2018). Therefore, the

Table 1
Comparison between the current study and state of the art of recent researches (February 2020) published on the application of standard and integrative machine learning methods in sediment transport modeling in rivers.

Study	Target variable	Machine learning methods
Choubin et al. (2018)	SSL	CART, ANN, SVM, ANFIS
Torabi and Dehghani (2018)	SSL	SVM, GEP
Yadav et al. (2018)	SSL	GA-SVM*, GA-ANN*
Yilmaz et al. (2018)	SSL	MARS
Rahgoshay et al. (2018)	SSL	GA-SVM*, M5Tree, MARS
Riahi-Madvar and Seifi (2018)	BL	ANN, ANFIS
Khosravi et al. (2018)	SSL	M5Tree
Liu et al. (2019)	SSL	Hilbert-Huang transform-ANN
Khan et al. (2019)	SSL	ANN
Kisi and Yaseen, 2019b	SSL	Evolutionary fuzzy model
Kumar et al. (2019)	SSL	ANN, ANFIS
Roushangar and Shahnazi (2019)	BL	ELM, PSO-ELM*
Sharghi et al. (2019a)	SSL	Emotional-ANN (EANN) hybrid Wavelet-EANN (WEANN)
Kaveh et al. (2020)	SSL	LSTM
The current study	SSL & BL	ANFIS, SVR, GA-ANFIS*, GA-SVR*

Note: SSL: Suspended Sediment Load; BL: Bedload; CART: Classification And Regression Tree; ANN: Artificial Neural Network; SVM: Support Vector Machine; ANFIS: Adaptive Neuro-Fuzzy Inference System; GEP: Gene Expression Programming; GA: Genetic Algorithm; MARS: multivariate adaptive regression splines; ELM: Extreme Learning Machine; PSO: Particle Swarm Optimization; LSTM: Long short Term Memory neural network; * = Integrative ML models.

performance assessment of the genetic algorithm integrated with machine learning models (i.e., SVR and ANFIS) in hydrological processes in sediment transport modeling can be mention as the contribution of the study.

2. Methods and methodology

The models applied in this study are divided into three groups: 1) traditional models including SRC and MLR, 2) standard ML models including ANIFS and SVR, and 3) integrated GA-SVR and GA-ANFIS models (see Fig. 1). The following sections describe the overall operation of each model.

2.1. Traditional models: SRC & MLR

A sediment rating curve (SRC) establishes a relationship between sediment discharge and stream discharge using a graph or equation and can be utilized for estimation of sediment loads using streamflow values (Asselman, 2000). The general form of the sediment rating curve can be written as:

$$S = aQ^b \tag{1}$$

where Q and S indicate stream discharge and sediment load, respectively. Also, a and b are the rating-curve parameters that the a-coefficient denotes the index of erosion severity and the coefficient indicates the erosive power of the river (Asselman, 2000). It can be mentioned that they can be obtained from the observed data using the regression process. By considering a linear regression, employing the correction factor is essential to avoid underestimation SSL values, however, in this study, a non-linear least squares regression is applied that the sediment load can be estimated at a specific value for stream discharge (Aytek and Kişi, 2008).

In addition to the traditional SRC mode, this study employs the statistical multiple linear regression (MLR) model to predict the dependent SSL/BL values by using input variables (X_1, X_2, …, X_n). In general, the MLR can be defined as (Rajaee et al., 2011):

$$Y_i = \beta_0 + \beta_1 X_{i1} + \beta_2 X_{i2} + \cdots + \beta_p X_{ip} + \varepsilon_i \tag{2}$$

where i *and* Y_i denote the number of observations and output variables (SSL/BL), respectively. β_i and ε_i indicate the coefficient of input variables and residual error, respectively. Note that for applying predictive MLR models, the input variables should be independent, and values of residual errors should be normally distributed (Šiljić Tomić et al., 2018). In the MLR modeling process, β values can be tuned by using observation values to find output values with a minimum error during training and testing phases. For this purpose, in this study, the least square approach (LSA) was used to calibrate the MLR model to minimize the difference between the predicted and observed values.

2.2. Adaptive neuro-fuzzy inference system (ANFIS)

Jang (1993) introduces the adaptive neuro-fuzzy inference system as a universal approximation approach. From the three common types of fuzzy inference systems, Tsukamoto's system, Sugeno's system, and Mamdani's system, the Sugeno first-order fuzzy method is more reliable than the others (Jang et al., 1997; Takagi and Sugeno, 1985). In this

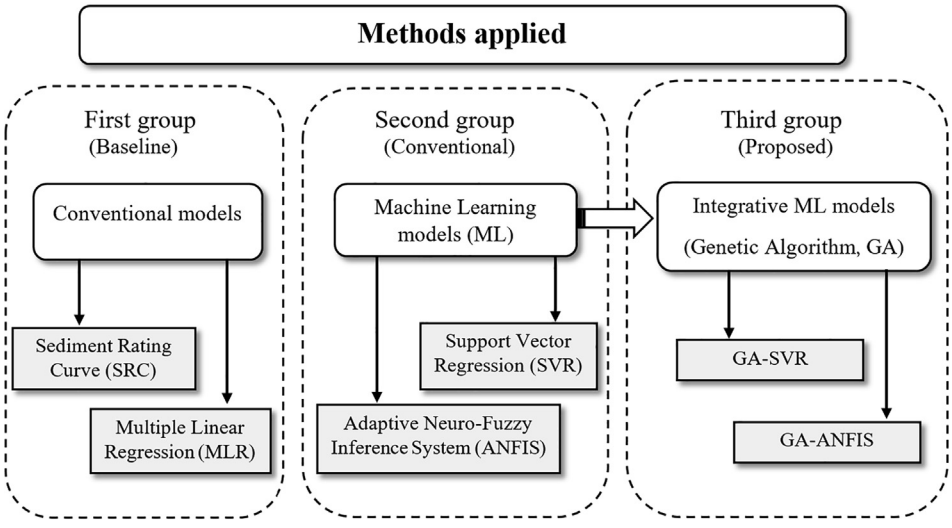

Fig. 1. Methods used to predict sediment load in the present study; the arrow leading from the second to the third group implies the integration of the standard ML models with the GA.

scheme, by applying two fuzzy IF/THEN statements, the following rules can be defined (Talei et al., 2010):

Rule 1: If x is A_1 and y is B_1, then $f_1 = p_1x + q_1y + r_1$ (3)

Rule 2: If x is A_2 and y is B_2, then $f_2 = p_2x + q_2y + r_2$ (4)

in which x and y are predictor variables and A_1, A_2, B_1, and B_2 values indicate membership indexes for x and y and p_1, q_1, r_1 and p_2, q_2, r_2 denote output function (f_1 and f_2) parameters. For establishing rules in the ANFIS model, grid partitioning and subtractive fuzzy clustering have been developed (Nayak et al., 2004). In this study, the fuzzy c-means (FCM) clustering approach is applied for constructing a relationship based on rules between predictor and predicted variables. Also, a combination of the least-squares and backpropagation gradient descent methods optimization is utilized for obtaining parameters of the membership functions (MFs) (Sanikhani et al., 2018). The general structure of an ANFIS is based on a multilayer network and consists of such connected nodes that the last layer computes the final output of the ANFIS model using the single node (Salih et al., 2019b). The equivalent ANFIS architecture is shown in Fig. 2a.

2.3. Support vector regression (SVR)

Support vector machines (SVMs), as robust classification approaches, have gained popularity in water resource management applications (Raghavendra and Deka, 2014). The SVM method has been suggested by (Cortes and Vapnik, 1995) and implemented based on statistical learning concepts. SVMs are applicable for solving both regression and classification problems. In this study, support vector regression (SVR) is used to find a relationship between an independent variable and dependent variable sets. The SVR is characterized by a two-layer network using nonlinear weights in the first and linear ones in the second layer. The estimator function of regression can be written as (Vapnik, 1998):

$$f(x) = \omega.\ \varphi(x) + b \tag{5}$$

where ω and b are a coefficient that should be obtained from the data and weight matrix, respectively, and ϕ(.) indicates inputs feature function. The values for ω and b can be calculated by minimizing the risk function:

$$r(C) = \frac{1}{2}\ \|\omega\|^2 + C\frac{1}{N}\sum_{i=1}^{N} L_\varepsilon(d_i, y_i) \tag{6}$$

where,

$$L_\varepsilon(d, y) = \begin{cases} |d - y| - \varepsilon & if\ |d - y| \geqslant \varepsilon \\ 0 & otherwise \end{cases} \tag{7}$$

in which $L_\varepsilon(d,y)$ and C denote the ε-insensitive loss function and the regularized index, respectively, and ε represents the tube size. For solving Eq. (7), it should be transformed into a constrained optimization expression as:

$$Minimize: \frac{1}{2}\ \|\omega\|^2 + C\left(\sum_{i=1}^{N} (\xi_i + \xi_i^*)\right) \tag{8}$$

$$Subject\ \ to \begin{cases} \omega_i\varphi(x_i) + b_i - d_i \leqslant \varepsilon + \xi_i^* & i = 1, 2, ...N \\ d_i - \omega_i\varphi(x_i) - b_i \leqslant \varepsilon + \xi_i & i = 1, 2, ...N \end{cases} \tag{9}$$

where ξ and ξ' are slack parameters. Constrained optimization can be solved using the Lagrangian mathematical technique and Karush–Kuhn–Tucker conditions. Also, it can be mentioned that in this study, the Gaussian kernel function is used. Fig. 2(b) shows the SVR model schematic representation.

2.4. Integration procedure of the integrative models

One of the main problem of the traditional optimization techniques is that they may drop in local optimum (Kisi et al., 2017). In this study to overcome this drawback, a reliable well-known evolutionary optimization approach, genetic algorithm (GA) which has been extensively used in water resource problems is applied to find the parameters of the ANFIS and SVR models. Due to the remarkable capabilities of GA, it can acquire a global optimal result to minimize error. In the next step, the optimized ANFIS and SVR models are utilized for both the SSL and BL simulation.

The GA is one of the heuristic search methods based on natural evolution process for solving nonlinear optimization problems that was developed by (Holland, 1975) and has been extensively applied in hydrological studies for enhancing the performance of soft computing models by minimizing the difference between predicted and observed values (Danandeh Mehr et al., 2018; Yaseen et al., 2019). The GA produces a set of a population (string) at the first stage and then evaluates the fitness index for each string by calculating the difference between observed and computed values using a fitness function. In the next stage, the new generation should be produced using a selection operation. In this study, the *Roulette wheel selection* strategy is applied to find the fittest individuals have more chance (individual fitness) to participate in the mating pool for establishing the next generation. In the crossover operation, the produced generation from the selection operator is used to create two child individuals by considering a degree of probability. Finally, the mutation operator ensures to avoid being trapped in local optima using the *polynomial mutation* method. More details about the GA can be found in (Ahmed and Sarma, 2005).

In this study, membership functions (MF) parameters of the integrative ANFIS model, and the kernel's constant parameters (the regularization parameter C and the insensitive loss coefficient ε) of the integrative SVR approach are determined by GA. In general, the process

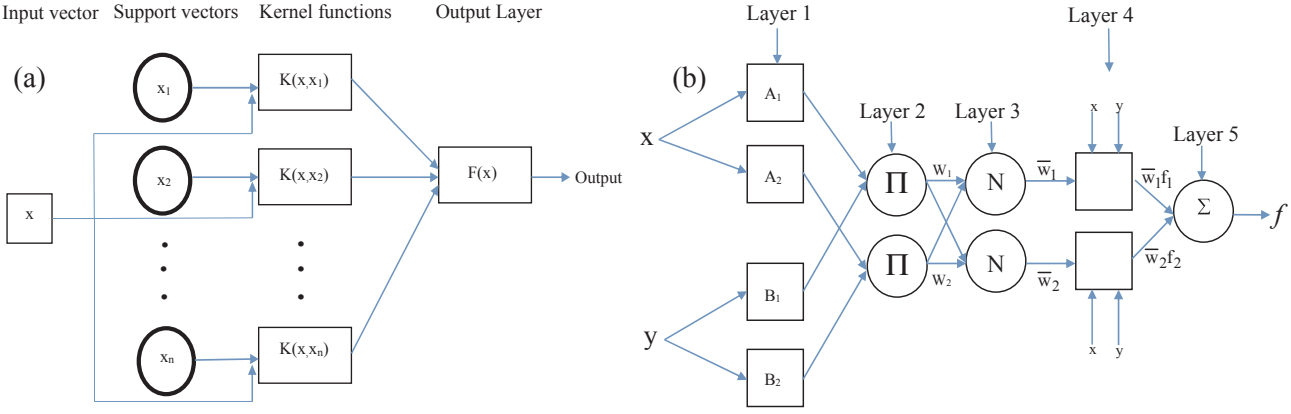

Fig. 2. (a) Equivalent ANFIS structure and (b) SVR model schematic representation.

Table 2
Initial given values for the GA parameters in integrative ML models.

Procedure	Parameters	value
Genetic algorithm	Mutation percentage	0.8
	Crossover percentage	0.7
	Selection pressure	8
	Mutation rate	0.5
Integrative GA-SVR	Population	10
	Maximum iteration	100
Integrative GA-ANFIS	Population	500
	Maximum iteration	1000

of applying GA to determine ANFIS and SVR parameters includes: 1) Creating the structure of SVR and ANFIS, 2) Initializing the GA parameters (see Table 2), 3) Creating a cost function to evaluate the fitness of the agents of population in each iteration, and, 4) executing the GA to determine optimization parameters in the integrative models. The employed procedure is shown in Fig. 3.

3. Case study and dataset

In this study, daily measured values of three hydrologic parameters including mean flow, suspended sediment and bedload data of a gauged station belonging to the Caguas Municipio basin on the Rio Grande de Loíza (drainage area = 232.6 km^2 and Gage datum 50.0 m above NGVD29) in Puerto Rico are used (Fig. 4). The Grande de Loíza is the largest river in Puerto Rico Island in volume and flows into the Atlantic Ocean. The data was downloaded from the web site of the United States Geological Survey (USGS Hydrologic Unit Code 21010005). The data length covers a five years long duration (1 January 1984 – 31 December 1988). The first four years of the daily datasets (80% of the data from 1/1/1984 to 31/12/1987) are assigned to the training data, and the data corresponds to the last year of the period (20% of datasets from 1/1/1988 to 31/12/1988) are used for evaluating the models' capabilities in terms of testing data. Fig. 5 shows the historical variation of the flow, SSL, and BL over the training and testing periods. Furthermore, descriptive statistical information for the applied datasets is presented in Table 3.

The descriptive statistics of data, including range, *mean*, and standard deviation (*Std.*) is given in Table 3. Table 3 clearly shows the magnitude of the difference between the flow, suspended sediment, and bedload values. It can be seen that the ranges of testing datasets fall into the ranges of training datasets. This fact confirms the validity of choosing the proper periods for the training and testing set so that the models will not encounter any unseen data (the data that does not fall into the training set domain) for the testing phase. In other words, the evaluation of the models will reflect their potential leaving no room for doubt about problems related to the existence of unseen data.

Considering the coefficient of variation values (*CV*), it can also be observed that the data distribution of SSL (CV = 8.5) and BL (CV = 6.7) values are much more dispersed than the flow data (CV = 2.7), which defines them as more sporadic phenomena than the flow rate series itself. Comparing the calculated correlation values between the flow rate and BL, as well as the flow rate and SSL, shows that flow data has less influence on BL rather than SSL. Besides, the zero *p*-values of the Run Test, for testing the randomness of a distribution, implies that the flow, SSL, and BL data series do not follow a particular predictable trend.

4. Performance measures and evaluation criteria

The present study evaluates the prediction capability of the applied models by using two deviance measures (including the Root Mean Square Error, *RMSE*) and the Mean Absolute Error, *MAE*), a similarity statistical measure (the coefficient of determination, R^2), and an efficiency measure (the Nash–Sutcliffe Efficiency, *NSE*). *RMSE* and *MAE* are among the best overall deviance statistical measures of model evaluation. According to Willmott and (Willmott and Matsuura, 2005), in comparison to the *MAE*, the *RMSE* is not a good criterion of average model performance; however, *MAE* is less sensitive to extreme data than *RMSE*. R^2 reflects the correlation between the observed and

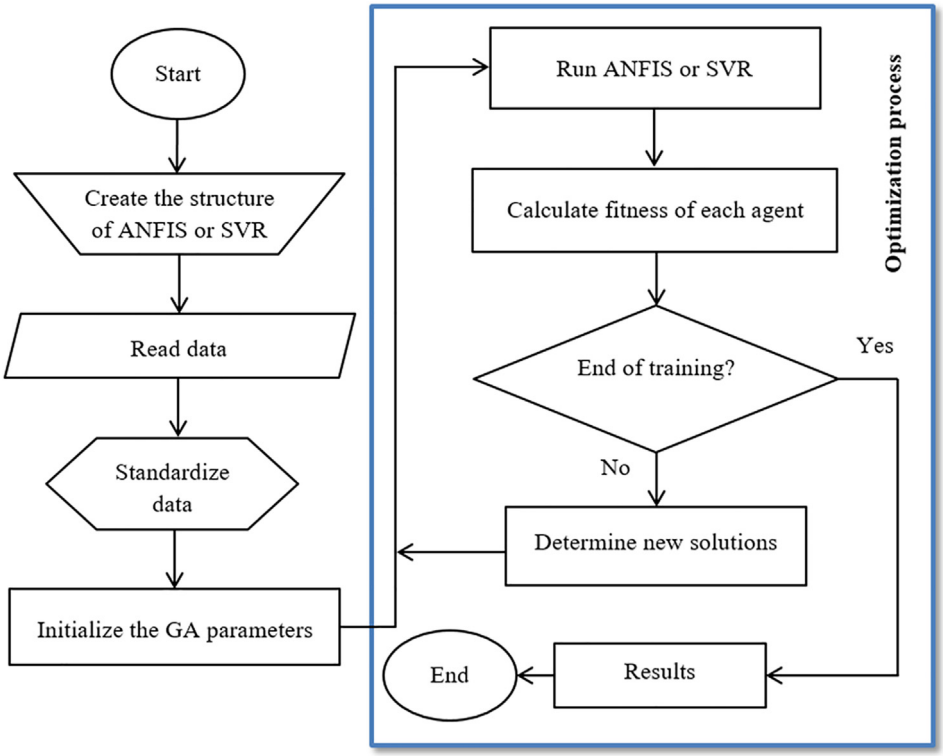

Fig. 3. The flowchart of the integration process of ANFIS and SVR models.

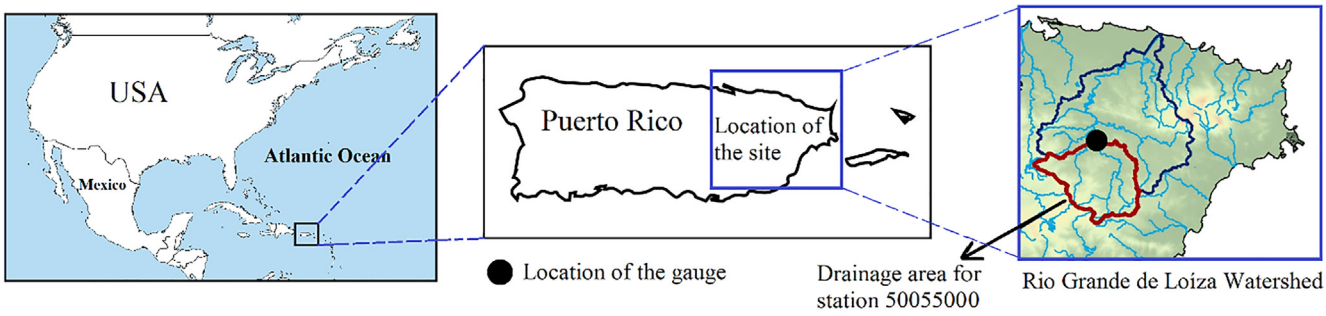

Fig. 4. Location map for the measuring gauge (adapted from *d-maps.com* and USGS website).

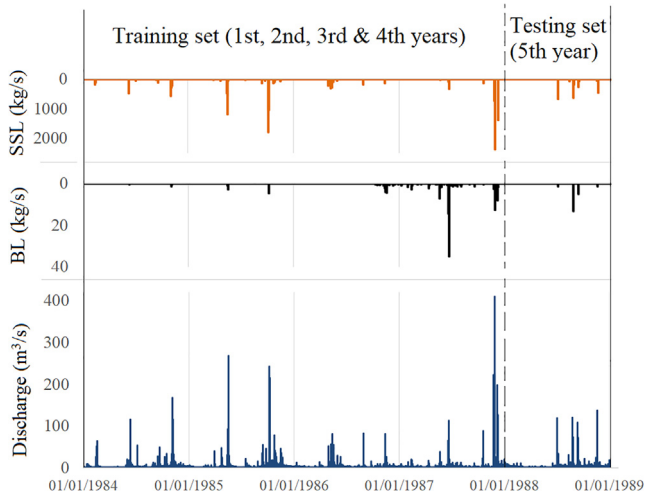

Fig. 5. Curves of time variation of observed daily flow, SSL, and BL for the training and testing periods.

modeled values, and a value of unity implies that the dispersion of the modeled values is equal to that of the observed data. It is worth noting that an under- or over-predict model might still result in good values for R^2 close to 1.0, even if all predictions are inaccurate. Thus, it is recommended to take into account an additional measure which can cope with this drawback. Hence, in this study, the *NSE* coefficient is considered as the fourth criterion for having a comprehensive appraisal of the models' performance (Elzwayie et al., 2016; Krause and Boyle, 2005). Mathematical formulations of the mentioned measures are written as below:

$$RMSE = \sqrt{\frac{\sum_{i=1}^{N}(S_M - S_O)^2}{N}}; \quad \text{Range} = [0, \infty), \quad \text{Ideal value} = 0 \tag{10}$$

$$MAE = \frac{1}{N}\sum_{i=1}^{N}|S_M - S_O|; \quad \text{Range} = [0, \infty), \text{Ideal value} = 0 \tag{11}$$

$$R^2 = \frac{\left(\sum_{i=1}^{N}(S_M - \bar{S}_M)(S_O - \bar{S}_O)\right)^2}{\sum_{i=1}^{N}(S_M - \bar{S}_M)^2 \sum_{i=1}^{N}(S_O - \bar{S}_O)^2}; \quad \text{Range} = [0, 1], \text{Ideal value} = 1 \tag{12}$$

$$NSE = 1 - \frac{\sum_{i-1}^{N}(S_M - S_O)^2}{\sum_{i-1}^{N}(S_O - \bar{S}_O)^2}; \quad \text{Range} = (-\infty, 1], \text{Ideal value} = 1 \tag{13}$$

where *So* is the observed value of SSL and BL (kg/s), S_M stands for the modeled (simulated/predicted) value of SSL and BL (kg/s) in the training/testing set, *N* is the number of the data samples, and bar denotes the mean value of the observed/modeled data.

5. Application analysis and results

The main objective of the current research is to investigate the capacity of integrative classical ML models, including ANFIS and SVR, with a nature-inspired optimization algorithm called genetic algorithm for modeling riverbed sediment load (BL) and suspended sediment load (SSL). The premier goal of developing such an integrative model is to overcome the hyperparameter associated problem. Based on the reported literature within the field of hydrology, the feasibility of the GA for tuning AI models demonstrated promising progress (Bozorg-Haddad et al., 2017; Ghorbani et al., 2018; Roushangar and Koosheh, 2015). The proposed integrative AI models were validated against the traditional sediment rating curve (SRC), multiple linear regression (MLR), and standalone ANFIS and SVR models.

Conceptually, in modeling river sediment, the river flow discharge (*Q*) is one of the essential hydrological processes that influences the sediment amount transport (Kisi and Yaseen, 2019). Hence, in this study, the prediction matrix of the applied predictive models is constructed based on the lead times of the correlated magnitudes of *Q* and the BL and SSL themselves. Note that the correlated lead values are determined using the statistical correlation following several studies

Table 3
Descriptive statistics for the daily river flow discharge, suspended sediment, and bedload data used in this study.

Period	Data	*Min*	*Max*	*Mean*	*Std.*	*CV*	*r* with Flow	*p*-value (Run Test)
Whole data	Flow (m^3/s)	0.54	410.59	7.41	20.06	2.71	1.00	0.00
	SSL (kg/s)	0.01	2383.46	11.61	98.40	8.47	0.92	0.00
	BL (kg/s)	0.00	34.95	0.19	1.26	6.68	0.48	0.00
Training set	Flow (m^3/s)	0.54	410.59	7.52	21.34	2.84	1.00	0.00
	SSL (kg/s)	0.01	2383.46	12.53	106.04	8.46	0.92	0.00
	BL (kg/s)	0.00	34.95	0.20	1.32	6.45	0.46	0.00
Testing set	Flow (m^3/s)	0.88	137.62	6.99	13.83	1.98	1.00	0.00
	SSL (kg/s)	0.02	700.34	7.96	58.52	7.35	0.91	0.00
	BL (kg/s)	0.00	13.52	0.13	0.98	7.86	0.68	0.00

Note: for p-value $<$ 0.05, the order of the data is considered to be random at 95% confidence level.

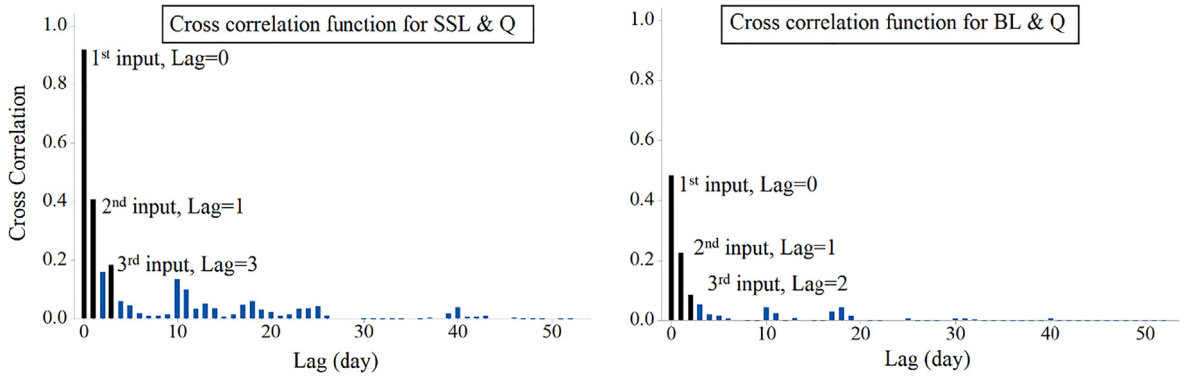

Fig. 6. The results of time-dependent statistical correlation between the BL & SSL and the river discharge.

Table 4
The constructed input variable combinations and modeling scenarios.

Modeling scenario	Models	Input/independent parameter(s)	Output parameter
I	SRC	Q(t)	SSL(t)
			BL(t)
	MLR-I	Q(t), Q(t-1), Q(t-3)	SSL(t)
	ANFIS-I	Q(t), Q(t-1), Q(t-2)	BL(t)
	SVR-I		
	GA-ANFIS-I		
	GA-SVR-I		
II	MLR-II	SSL(t-1), SSL(t-3), Q(t), Q(t-1), Q(t-3)	SSL(t)
	ANFIS-II		
	SVR-II	BL(t-1), BL(t-2), Q(t), Q(t-1), Q(t-2)	BL(t)
	GA-ANFIS-II		
	GA-SVR-II		

conducted over the literature (Afan et al., 2014; Kisi, 2012) (Fig. 6). The constructed input combinations are tabulated in Table 4. It can be noticed from Table 4 that there are two types of scenarios, Input I: Incorporated only the river discharge information; whereas, Input II: Incorporated the river discharge and sediment information for the BL and SSL. It is worth noting that in real-world modeling, the first input scenario is more practical than the second scenario.

5.1. Suspended sediment load modeling results

Table 5 reports the statistical results of the applied proposed integrative ML models (GA-ANFIS and GA-SVR) as well as traditional and conventional ML models for both modeling scenarios over the training phase. For the evaluation purpose, the minimal absolute error measures (i.e., *RMSE* and *MAE*), the model efficiency (i.e., *NSE*), and best-fit-goodness measure (i.e., R^2) are considered. In general, the determination coefficient (R^2) revealed good performance for all models as per the reported research (Moriasi et al., 2007). The training prediction exhibits a variance predictability capacity, and this is observable over the proposed modeling scenarios (Table 5). This can be justified due to the sufficiency of the data span used for the learning process. However, the integrative AI models (GA-*models*) demonstrate the superior potential for training the predictive models (26% to 54% improvement in *MAE* values, see Table 5). Apparently, this is due to the efficiency of nature-inspired optimization algorithms where the appropriate tuning internal parameters were allocated for the ANFIS and SVR models. It is worth highlighting that the lowest prediction performance was attained using the traditional approaches, which is a normal outcome following several established pieces of research over the literature (Rajaee et al., 2011).

The potential of the applied predictive models for modeling SSL over the testing phase and for both modeling scenarios is reported in Table 6 and Fig. 7. The statistical performances demonstrate a variance between all models and over both the modeling scenarios of the input variables. In other words, the evidence reveals the superiority of the integrative ML models (i.e., GA-ANFIS and GA-SVR) over the traditional and conventional ML models.

For instance, combining the GA algorithm with the SVR-I model (*RMSE* of GA-SVR-I = 18.670) improves the *RMSE* values of SVR-I (*RMSE* of GA-SVR = 19.896) up to 1.123 kg/s. Overall, the GA-ANFIS-II model (with minimal *RMSE* = 16.82 kg/s and maximal *NSE* = 0.918) and GA-SVR-II (with the best equilibrium values for *NSE* = 0.905,

Table 5
The performance indicators of the SSL modeling over the training phase.

Category	Model-Scenario	*RMSE* (kg/s)	R^2	*MAE* (kg/s)	*NSE*	*MAE* improvement
Traditional models	SRC	28.309	0.930	6.448	0.930	Base
	MLR-I	37.244	0.877	15.014	0.877	−132.85
	MLR-II	36.399	0.882	13.682	0.882	−112.19
Conventional ML models	ANFIS-I	26.812	0.936	5.486	0.936	14.92
	ANFIS-II	17.295	0.973	3.959	0.973	38.60
	SVR-I	32.606	0.943	3.415	0.902	47.04
	SVR-II	34.773	0.928	3.658	0.893	43.27
Integrative ML models	GA-ANFIS-I	26.482	0.938	4.719	0.938	26.81
	GA-ANFIS-II	13.936	0.983	3.213	0.983	50.17
	GA-SVR-I	19.898	0.973	2.879	0.963	55.35
	GA-SVR-II	24.980	0.945	2.942	0.945	54.37

Table 6
The performance indicators of the SSL prediction over the testing phase.

Category	Model-Scenario	*RMSE* (kg/s)	R^2	*MAE* (kg/s)	*NSE*	*MAE* improvement
Traditional models	SRC	20.945	0.894	5.942	0.872	Base
	MLR-I	25.254	0.857	12.291	0.814	−106.85
	MLR-II	24.196	0.863	11.332	0.83	−90.71
Conventional ML models	ANFIS-I	20.871	0.893	5.327	0.873	10.35
	ANFIS-II	18.421	0.934	5.798	0.901	2.42
	SVR-I	19.896	0.911	2.602	0.885	56.21
	SVR-II	19.694	0.911	2.706	0.887	54.46
Integrative ML models	GA-ANFIS-I	19.974	0.906	4.675	0.884	21.32
	GA-ANFIS-II	16.82	0.931	4.011	0.918	32.50
	GA-SVR-I	18.670	0.910	2.626	0.898	55.81
	GA-SVR-II	18.028	0.906	2.809	0.905	52.73

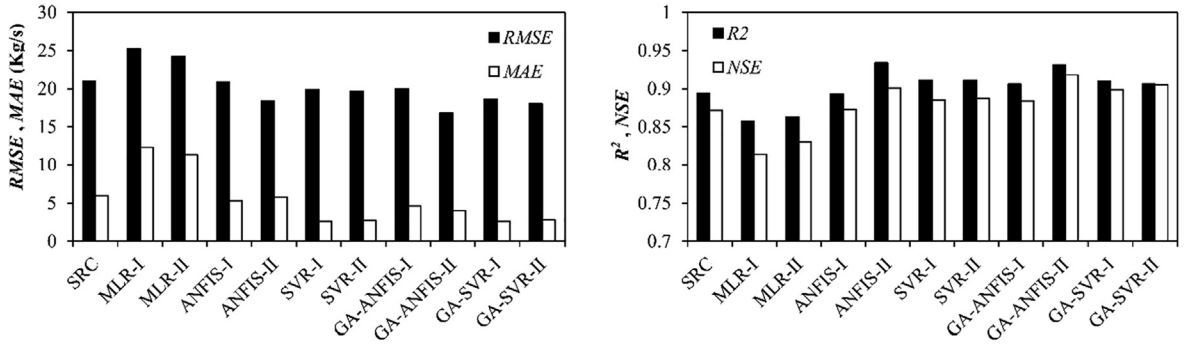

Fig. 7. *RMSE* and *MAE* error histograms as well as R^2 and *NSE* histograms for the predicted SLL values.

MAE = 2.809 kg/s, and *RMSE* = 18.02 kg/s) acted better than the other applied models. It is worth to mention that the determination coefficient indicator is not efficient here to demonstrate the predictability performance presentation. Hence, a combination of evaluation indicators (e.g., *RMSE*, *MAE*, *NSE*, and R^2), provides a meaningful opportunity to evaluate the developed predictive models.

5.2. Bedload modeling results

The statistical performance of the BL modeling over the training and testing phases using all of the applied predictive models is tabulated in Tables 7 and 8, respectively. One major observation in the reported statistical performances is the considerable difference between the R^2 values for the first input combinations (scenario I) and second input combinations (scenario II). For instance, the MLR-I has an R^2 = 0.212, whereas the MLR-II has an improved R^2 = 0.530 (see Table 7). The same trend can be observed, more or less, for the other models. However, one should note that R^2 sometimes fails to give an informative evaluation for the prediction accuracy (Yaseen et al., 2016). Hence, a combination of indicators should be established for the modeling evaluation. On the other hand, it can clearly be seen that the SRC and MLR-I models perform poorly according to the *RMSE*, R^2, *MAE*, and *NSE* criteria (see Tables 7 and 8). Over the training phases, the integrative GA-SVR-II model using the second modeling scenario input variability was accomplished the minimal absolute error measures value (*RMSE* = 0.53 kg/s and *MAE* = ≈0.074 kg/s). Over the testing phase, the integrative GA-ANFIS-II, using the second modeling scenario, demonstrates the best accuracy in terms of *RMSE* = 0.53 *kg/s*, R^2 = 0.72, *NSE* = 0.714, and 42.6% *MAE* improvement, while GA-SVR-II provides the lowest value for *MAE* = 0.061 kg/s and 72.7% *MAE* improvement. It can be also concluded that taking into account the sediment information in the second input scenario (*models*-II) noticeably improves the prediction capabilities of the applied models (Tables 6 and 8 and Fig. 8).

Table 7
The performance indicators of the BL modeling over the training phase.

Category	Model-Scenario	*RMSE* (kg/s)	R^2	*MAE* (kg/s)	*NSE*	*MAE* improvement
Traditional models	SRC	1.174	0.213	0.268	0.212	Base
	MLR-I	1.172	0.212	0.249	0.212	7.09
	MLR-II	0.905	0.530	0.184	0.53	31.34
Conventional ML models	ANFIS-I	1.068	0.346	0.244	0.346	8.96
	ANFIS-II	0.841	0.594	0.185	0.594	30.97
	SVR-I	1.237	0.371	0.167	0.123	37.69
	SVR-II	0.492	0.861	0.101	0.861	62.31
Integrative ML models	GA-ANFIS-I	0.936	0.498	0.227	0.498	15.30
	GA-ANFIS-II	0.593	0.799	0.183	0.799	31.72
	GA-SVR-I	0.896	0.659	0.135	0.142	49.63
	GA-SVR-II	0.485	0.866	0.074	0.865	72.39

Table 8
The performance indicators of the BL prediction over the testing phase.

Category	Model-Scenario	*RMSE* (kg/s)	R^2	*MAE* (kg/s)	*NSE*	*MAE* improvement
Traditional models	SRC	0.778	0.463	0.223	0.377	Base
	MLR-I	0.773	0.468	0.192	0.385	13.90
	MLR-II	0.693	0.507	0.146	0.506	34.53
Conventional ML models	ANFIS-I	0.720	0.553	0.159	0.466	28.70
	ANFIS-II	0.616	0.614	0.161	0.609	27.80
	SVR-I	0.814	0.446	0.092	0.439	58.74
	SVR-II	0.644	0.575	0.098	0.573	56.05
Integrative ML models	GA-ANFIS-I	0.649	0.630	0.192	0.566	13.90
	GA-ANFIS-II	0.527	0.721	0.128	0.714	42.60
	GA-SVR-I	0.798	0.438	0.083	0.569	62.78
	GA-SVR-II	0.611	0.638	0.061	0.615	72.65

5.3. Incorporative diagnostic analysis

For having a better and comprehensive visualization, the proposed, traditional, and conventional predictive models are evaluated graphically using scatterplots over the testing phase, as reported in Figs. 9 and 10 for SSL and BL, respectively. In these figures, the best predictive models were displayed for better understanding. Based on the reported graphical presentation for SSL prediction, the highest correlation and best match between the measured and predicted values are attained using the integrative GA-ANFIS and the standalone ANFIS models using the second modeling scenario input variability. This can be best explained due to the high stochasticity pattern of the SSL, which requires informative hydrological variables for capturing the complexity of the SSL system (e.g., river discharge). Hence, the incorporation of the antecedent values of SSL improves the accuracy of predicted SLL values. The attained correlation coefficient values for the GA-ANFIS-II and ANFIS-II models are slightly similar (r = 0.96). It should be noted, although the highest correlation obtained for the GA-ANFIS-II and ANFIS-II models; however, these two models demonstrate a noticeable overestimation trend for the minimal sediment magnitudes. On the contrary, a more coherent prediction agreement for the integrative GA-SVR and standalone SVR can be observed over both modeling scenarios. Fig. 10 illustrates the scatterplots trend for the BL sediment prediction. A consistent predictability performance can be observed for the integrative ANFIS-GA-II model for predicting BL sediment with the highest correlation coefficient (r = 0.85). However, a remarkable diversion from the best fit-line for all models toward the over-estimation manners can be distinguished except for the attained results using the integrative GA-SVR_II model (r = 0.79). It is worth to mention, the

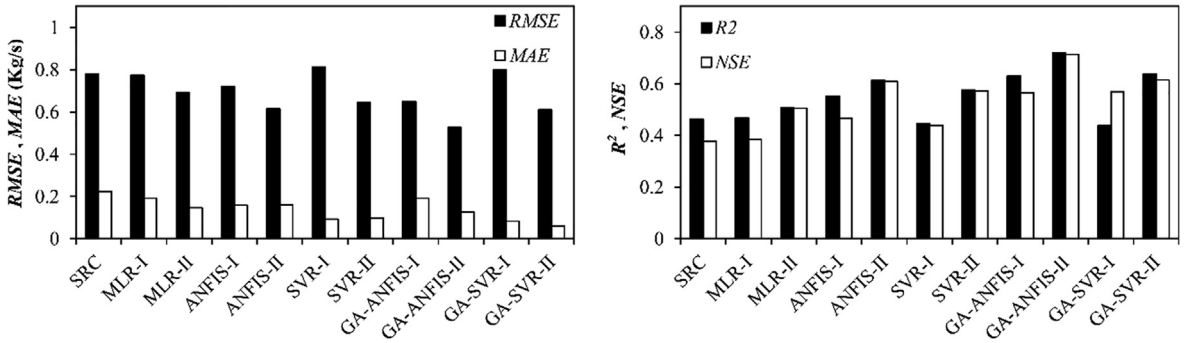

Fig. 8. *RMSE* and *MAE* error histograms as well as R^2 and *NSE* histograms for the predicted BL values.

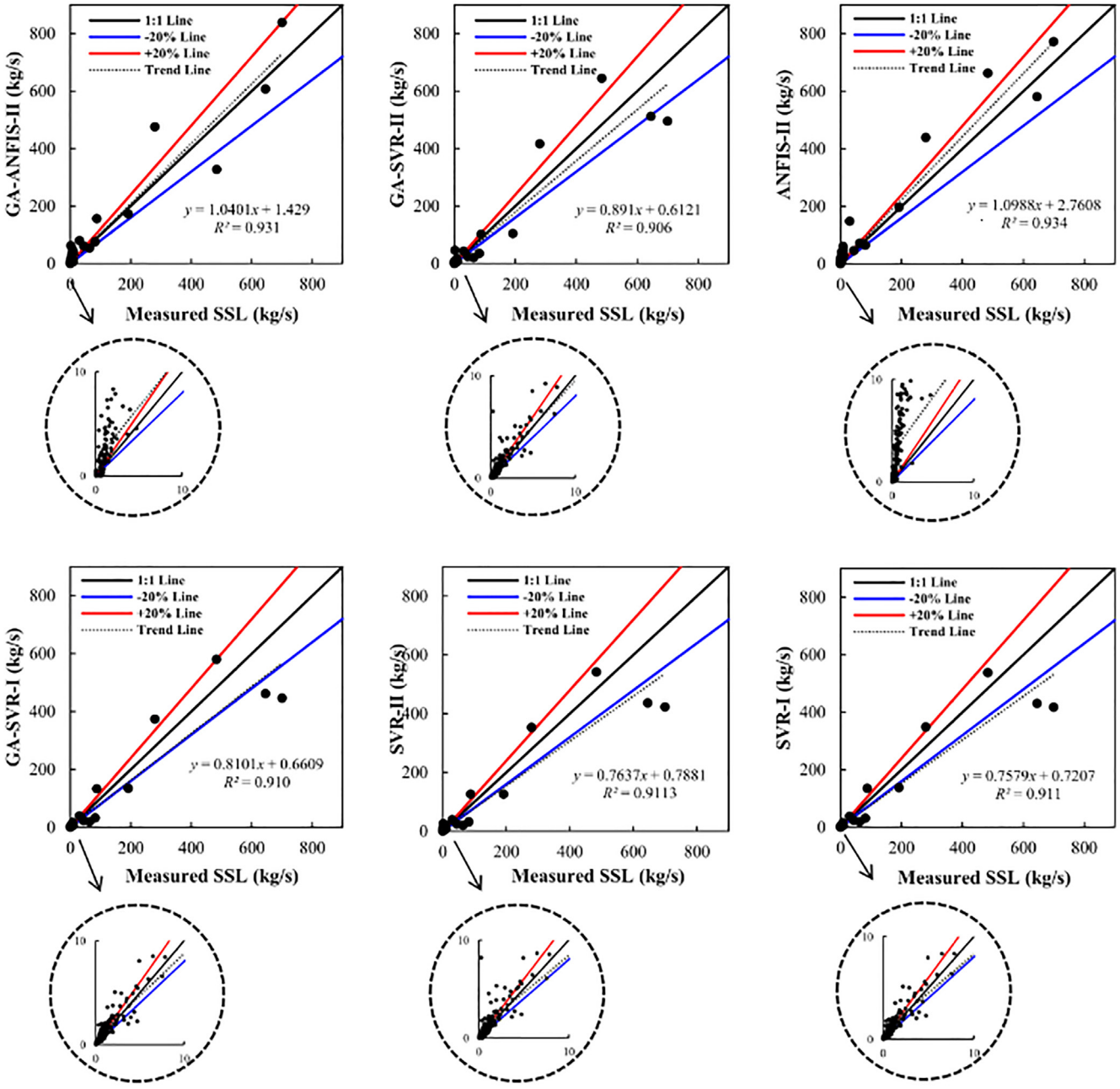

Fig. 9. Scatter plots of observed versus predicted SSL values.

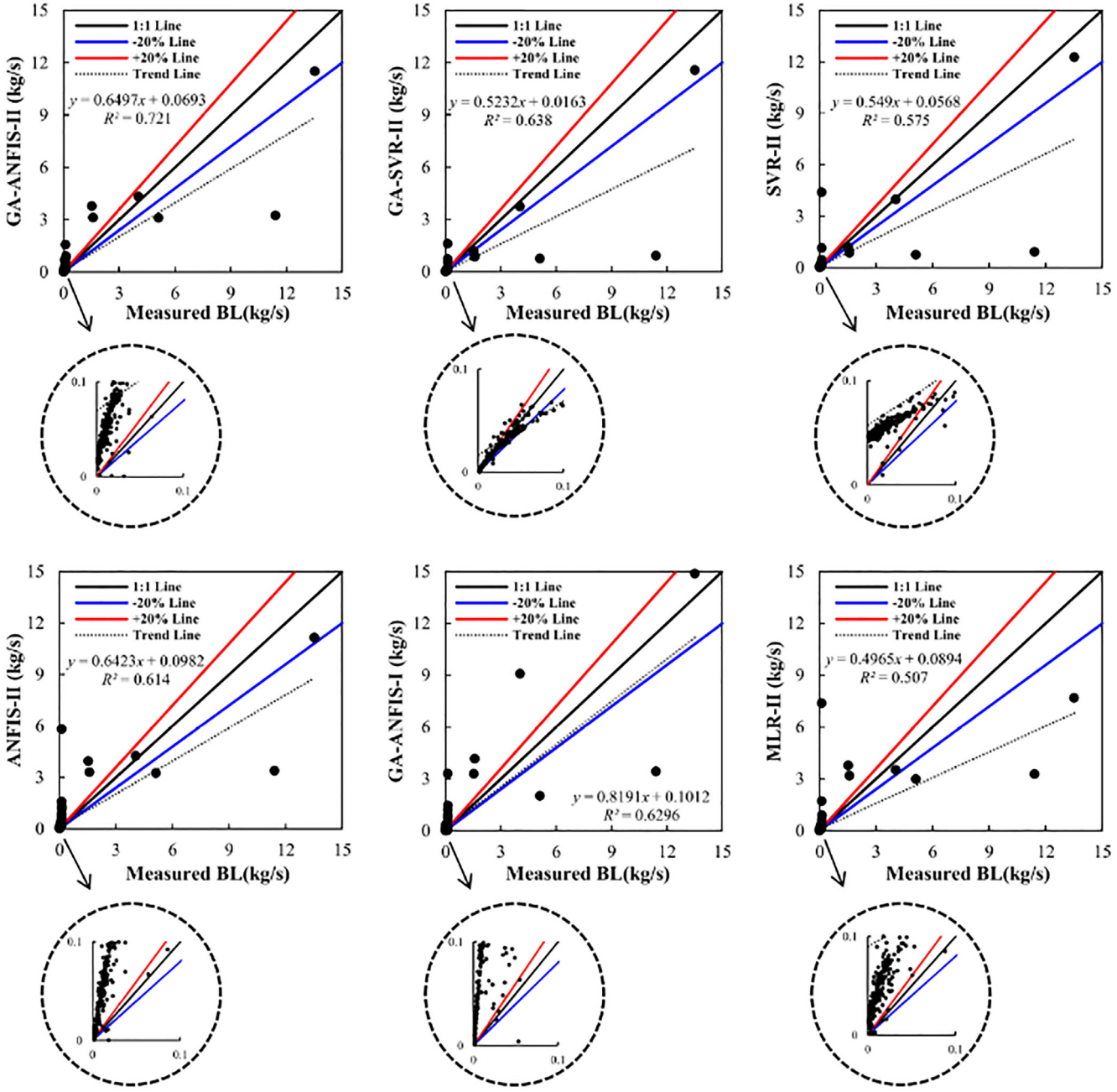

Fig. 10. Scatter plots of observed versus predicted BL values.

applied predictive models failed to predict the high magnitudes of the sediments for both SSL and BL. This is apparently owing to the sudden changes in the river discharge amount. This is due to high rainfall intensity events that generate land sliding phenomena. Hence, the applied models apparently demonstrated an observable limitation toward those high magnitudes of sediment loads. Another explanation for this limitation, the developed predictive models did not experience those high magnitudes of sediment for both SSL and BL during the training modeling phase and thus failed to mimic the actual mechanism between the predictors and predictand variables. Note that, this is a time series sequential hydrological process where random periodic modeling development cannot be established here. This can be better understood through the incorporation of the casual hydrological variables such as climatological, hydraulic characteristics, or other related essential hydrological variables as external predictors for better prediction matrix.

Fig. 11 displays the 2-dimensional graphical presentation, called the Taylor diagram, for the developed predictive models for the SSL and BL, respectively. Taylor diagram is one of the best graphical visualizations to evaluate the prediction accuracy based on several statistical indicators (Taylor, 2001). It presents the summary statistical indicators of the measured and predicted sediment, including correlation coefficients, standard deviations, and root mean square error. In other words, the Taylor diagram provides an excellent graphical representation of the similarity between the predicted and observed values. Fig. 11 reveals the slightly similar performance of the applied predictive models for both modeling input scenarios. However, the proposed integrative GA-ANFIS-II and GA-SVR-II indicate the closest coordinates to the measured SSL. On the other hand, Fig. 11 indicates that GA-ANFIS-II is the best predictive model toward the measured BL benchmark.

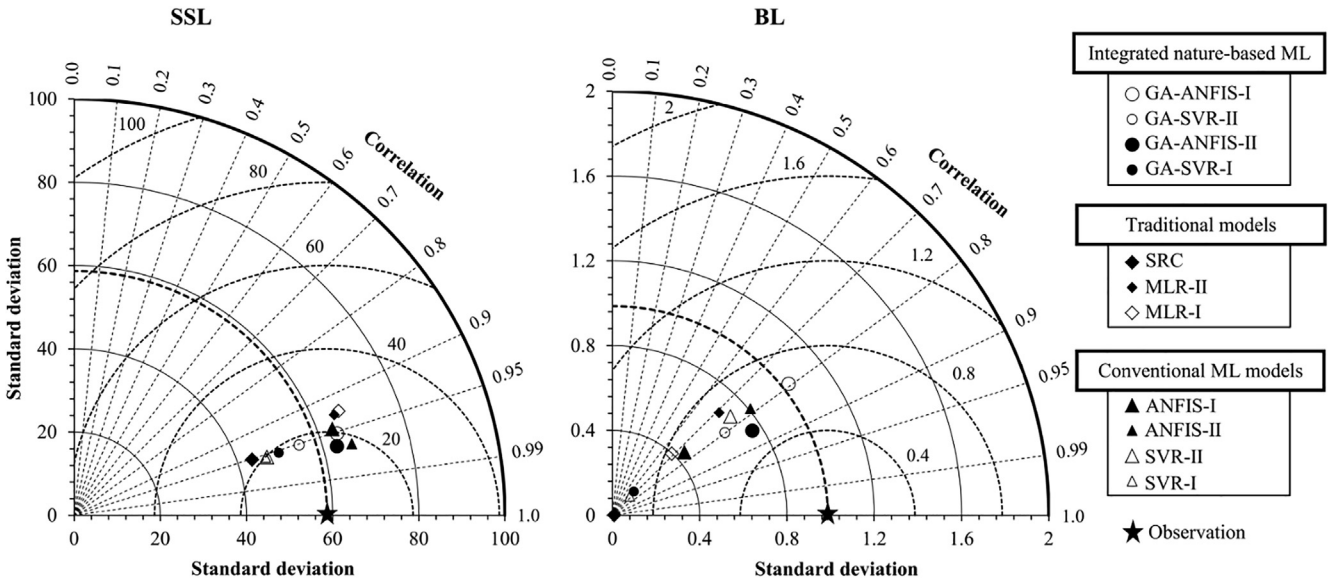

Fig. 11. Taylor Diagram for the applied predictive models for the two modeling scenarios (I and II) as well as the types of the river sediments (SSL and BL).

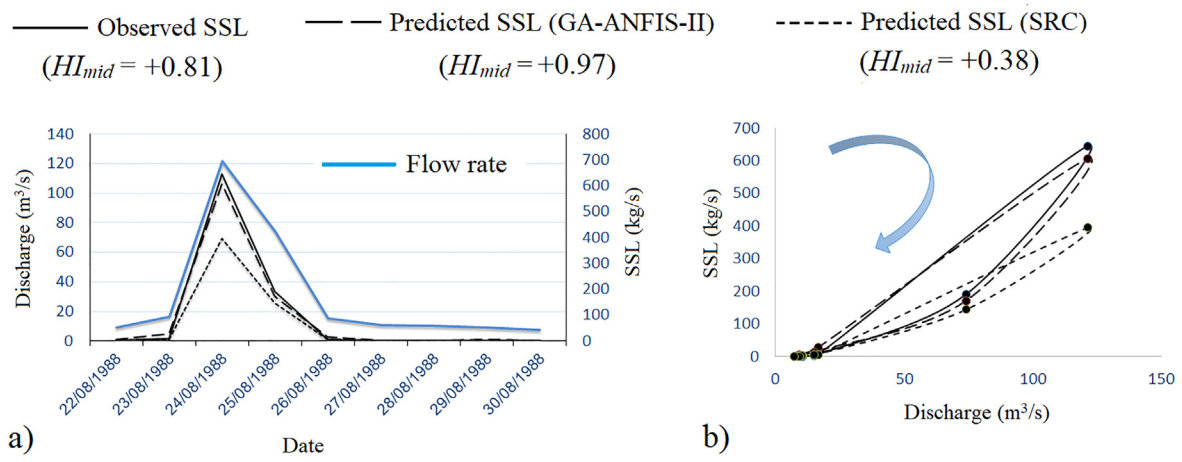

Fig. 12. a) Comparing the observed versus predicted results of the suspended sediment load during a flood; b) hysteresis curves for the SSL for the same flood and calculated HI_{mid} values.

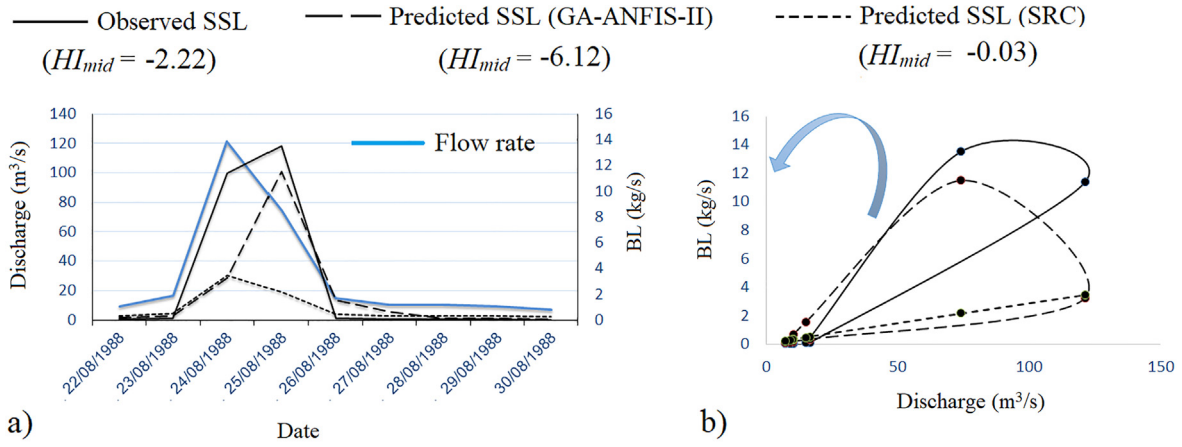

Fig. 13. a) Comparing the observed versus predicted results of the bedload during a flood; b) hysteresis curves for the BL for the same flood and calculated HI_{mid} values.

6. Deliberation and discussion

From the results of this study, it was found that irrespective of the method used, the prediction of SSL was reasonably accurate by all the methods (with an R^2 ranging from 0.857 to 0.934 and *NSE* ranging from 0.814 to 0.918 for the testing data for all of the applied models). Despite the use of ML techniques or their variants, the predictability of BL is less accurate than the SSL, which is a major concern for the modelers. Along with the inclusion of appropriate parameter sets, a considerable amount of effort is required in the model development phase. Further examination and deliberation for the attained results of the models can be achieved by the use of hysteresis analysis. Hysteresis analysis is a promising graphical tool for studying the non-linear relationship between sediment concentration and fluvial discharge (Lloyd et al., 2016). It is basically plotted between sediment load and fluvial discharge. In this study, a flood hydrograph in the testing phase from 22/08/1988 to 30/08/1988 is considered for the hysteresis analysis of both SSL and BL. The flood hydrograph, hysteresis loop of observed SSL, and hysteresis loops of SSL predicted by the best integrative model and the basic SRC models are presented in Fig. 12. The corresponding plots for BL are also provided in Fig. 13. The properties of the loop can be quantified by its primary characteristic property mean hysteresis index (HI_{mid}), which effectively shows the dynamic response of suspended sediment concentrations to flow changes during storm events. The HI_{mid} index estimates the fatness of the hysteresis loop corresponds to the mid-point discharge of the flood hydrograph (Eqs. (14) and (15)) (Lawler et al., 2006).

$$HI_{mid} = \left(\frac{S_R}{S_F}\right) - 1;\ \text{Clockwise} \tag{14}$$

$$HI_{mid} = -1/\left(\frac{S_R}{S_F}\right) + 1;\ \text{Anti - clockwise} \tag{15}$$

In the above formulae, S stands for sediment load, which can be either bedload or suspended load, R stands for rising limb, and F stands for falling limb. $HI_m \approx 0$ indicates a weak hysteresis loop, a positive value indicates a clockwise loop, and a negative value indicates an anticlockwise loop. The computed HI_{mid} values are given in Figs. 12 and 13. Figs. 12 and 13 show that for the SSL, the hysteresis loop is clockwise, while for BL, it is anti-clockwise in nature. The clockwise hysteresis loop is formed due to an increasing concentration of sediment that forms more rapidly during rising limb, which suggests a source of sediment close to the monitoring point and sediment depletion in the channel system (Baniya et al., 2019). On the contrary, an anticlockwise hysteresis loop shows a long gap between the discharge and concentration peak, which suggests that the source is located far from the monitoring point or bank collapse (Lloyd et al., 2016). As for the SSL modeling, it is clear from Fig. 12 that the GA-ANFIS-II model displays excellent predictability, and the hysteresis loop of ANFIS-GA based predictions shows striking similarity with that of observed values ($HI_{mid} = +0.81$ vs. $+0.97$). The hysteresis loop of SRC based predictions shows a significant deviation from that of the observed data, which indicates poor predictability power of the SRC model ($HI_{mid} = +0.38$).

Hysteresis analysis for the BL model can be seen in Fig. 13. Fig. 13 implies that the GA-ANFIS-II model shows fair performance in the prediction of the BL correctly, while the SRC method could not simulate the BL of the river system well. Although there is a considerable difference between the calculated HI_{mid} values for the observed loop and predicted GA-ANFIS-II's loop (-2.22 vs. -6.12), this illustration clearly depicts that the ML model (GA-ANFIS) was successful in regenerating the hysteresis loop. In contrast, the SRC failed in capturing the loop (Fig. 13). That is, the corresponding HI_{mid} value for the SRC model is -0.03, which is close to zero and indicates no loop at all.

It is noteworthy that the data length in the present work covers five consecutive years from 1984 to 1989. Thus, the results obtained here are confined to a moderate time-series dataset, so more future works are needed for reaching holistic feedback on the merits of the usage of integrative ML models in BL and SSL prediction.

7. Conclusions

This study performed a systematic evaluation of complexities in suspended sediment load (SSL) and bedload (BL) prediction in river flow through a multitude of statistical and machine learning (ML) methods. The predictive methods included traditional models (SRC & MLR), conventional ML models (SVR & ANFIS), and integrative ML models (GA-SVR & GA-ANFIS). The applied models were constructed based on the flow rate discharge data, and by considering two different input scenarios: with and without past records of sediment data.

From the major findings of this study, the following general observations can be pointed out: (i) the predictability of SSL was better than the prediction of BL irrespective of the model applied; (ii) SRC and conventional models showed poor performance in prediction of both SSL and BL; (iii) the inclusion of lagged inputs of sediment was more effective in improving the predictability of the SSL than BL; (iv) regardless of the input scenarios, the machine learning models were superior to the traditional methods in prediction of SSL and BL, and, (v) a blatant improvement in predicting ability of integrative ML models could be observed in comparison to the standard ML models (an average improvement of 7% of *RMSE* and 10% of R^2). Indeed, the current study showed that ML models could be successfully employed to simulate and predict the nonlinear river SSL process in situations where both temporal river flow and sediment data are available. However, considering the complex nature of the bedload (BL) time series, the utilization of the ML methods can be more beneficial by having access to extra physiographical information, such as landslide susceptibility maps of the watershed.

CRediT authorship contribution statement

Mohammad Zounemat-Kermani: Writing - original draft, Writing - review & editing, Formal analysis. **Amin Mahdavi-Meymand:** Data curation, Software, Formal analysis. **Meysam Alizamir:** Writing - original draft, Writing - review & editing, Methodology. **S. Adarsh:** Writing - original draft, Writing - review & editing. **Zaher Mundher Yaseen:** Writing - original draft, Writing - review & editing.

Declaration of Competing Interest

The authors declare that they have no known competing financial interests or personal relationships that could have appeared to influence the work reported in this paper.

References

Adnan, Liang, El-Shafie, Zounemat-Kermani, Kisi, 2019. Prediction of suspended sediment load using data-driven models. Water 11, 2060. https://doi.org/10.3390/w11102060.

Afan, H.A., El-Shafie, A., Yaseen, Z.M., Hameed, M.M., Mohtar, W.H.M.W., Hussain, A., 2015. ANN based sediment prediction model utilizing different input scenarios. Water Resour. Manage. 29, 1231–1245.

Afan, H.A., El-Shafie, A., Yaseen, Z.M., Hameed, M.M., Wan Mohtar, W.H.M., Hussain, A., 2014. ANN based sediment prediction model utilizing different input scenarios. Water Resour. Manage. 29, 1231–1245. https://doi.org/10.1007/s11269-014-0870-1.

Ahmed, J.A., Sarma, A.K., 2005. Genetic algorithm for optimal operating policy of a multipurpose reservoir. Water Resour. Manage. 19, 145–161. https://doi.org/10.1007/s11269-005-2704-7.

Asselman, N.E.M., 2000. Fitting and interpretation of sediment rating curves. J. Hydrol. https://doi.org/10.1016/S0022-1694(00)00253-5.

Aytek, A., Kişi, Ö., 2008. A genetic programming approach to suspended sediment modelling. J. Hydrol. 351, 288–298. https://doi.org/10.1016/j.jhydrol.2007.12.005.

Azamathulla, H.M., Ab. Chang, C.K., Ghani, A., Ariffin, J., Zakaria, N.A., Abu Hasan, Z., 2009. An ANFIS-based approach for predicting the bed load for moderately sized

rivers. J. Hydro-Environ. Res. 3, 35–44. https://doi.org/10.1016/j.jher.2008.10.003.
Baniya, M.B., Asaeda, T.K.C.S., Jayashanka, S.M.D.H., 2019. Hydraulic Parameters for Sediment Transport and Prediction of Suspended Sediment for Kali Gandaki River Basin, Himalaya. Nepal. Water 11, 1229. https://doi.org/10.3390/w11061229.
Bozorg-Haddad, O., Soleimani, S., Loáiciga, H.A., 2017. Modeling water-quality parameters using genetic algorithm-least squares support vector regression and genetic programming. J. Environ. Eng. 143, 04017021. https://doi.org/10.1061/(asce)ee.1943-7870.0001217.
Chang, C.K., Azamathulla, H.M.D., Zakaria, N.A., Ghani, A.A.B., 2012. Appraisal of soft computing techniques in prediction of total bed material load in tropical rivers. J. Earth Syst. Sci. 121, 125–133. https://doi.org/10.1007/s12040-012-0138-1.
Choubin, B., Darabi, H., Rahmati, O., Sajedi-Hosseini, F., Kløve, B., 2018. River suspended sediment modelling using the CART model: a comparative study of machine learning techniques. Sci. Total Environ. 615, 272–281. https://doi.org/10.1016/j.scitotenv.2017.09.293.
Cortes, C., Vapnik, V., 1995. Support-vector networks. Mach. Learn. 20, 273–297. https://doi.org/10.1023/A:1022627411411.
Danandeh Mehr, A., Nourani, V., Kahya, E., Hrnjica, B., Sattar, A.M.A., Yaseen, Z.M., 2018. Genetic programming in water resources engineering: a state-of-the-art review. J. Hydrol. https://doi.org/10.1016/j.jhydrol.2018.09.043.
Elzwayie, A., El-shafie, A., Yaseen, Z.M., Afan, H.A., Allawi, M.F., 2016. RBFNN-based model for heavy metal prediction for different climatic and pollution conditions. Neural Comput. Appl. https://doi.org/10.1007/s00521-015-2174-7.
Fan, J., Yao, Q., 2008. Nonlinear Time Series: Nonparametric and Parametric Methods. Springer Science & Business Media.
Ghorbani, M.A., Khatibi, R., Mehr, A.D., Asadi, H., 2018. Chaos-based multigene genetic programming: a new hybrid strategy for river flow forecasting. J. Hydrol. 562, 455–467.
Haddadchi, A., Movahedi, N., Vahidi, N., Omid, M.H., Dehghani, A.A., 2013a. Evaluation of suspended load transport rate using transport formulas and artificial neural network models (Case study: Chelchay Catchment). J. Hydrodyn. 25, 459–470.
Haddadchi, A., Omid, M.H., Dehghani, A.A., 2013b. Bedload equation analysis using bed load-material grain size. J. Hydrol. Hydromech. 61, 241–249. https://doi.org/10.2478/johh-2013-0031.
Haddadchi, A., Omid, M.H., Dehghani, A.A., 2012. Assessment of bed-load predictors based on sampling in a gravel bed river. J. Hydrodyn. https://doi.org/10.1016/S1001-6058(11)60229-1.
Holland, J., 1975. Adaptation in Natural and Artificial Systems. University of Michigan Press, Ann Arbor.
Jang, J.-S.R., Sun, C.-T., Mizutani, E., 1997. Neuro-Fuzzy and Soft Computing: A Computational Approach to Learning and Machine Intelligence. Prentice Hall.
Kakaei Lafdani, E., Moghaddam Nia, A., Ahmadi, A., 2013. Daily suspended sediment load prediction using artificial neural networks and support vector machines. J. Hydrol. https://doi.org/10.1016/j.jhydrol.2012.11.048.
Kaveh, K., Kaveh, H., Bui, M.D., Rutschmann, P., 2020. Long short-term memory for predicting daily suspended sediment concentration. Eng. Comput. 1–15.
Khan, M.Y.A., Tian, F., Hasan, F., Chakrapani, G.J., 2019. Artificial neural network simulation for prediction of suspended sediment concentration in the River Ramganga, Ganges Basin, India. Int. J. Sedim. Res. 34, 95–107. https://doi.org/10.1016/j.ijsrc.2018.09.001.
Khosravi, K., Mao, L., Kisi, O., Yaseen, Z.M., Shahid, S., 2018. Quantifying hourly suspended sediment load using data mining models: case study of a glacierized Andean catchment in Chile. J. Hydrol. 567, 165–179. https://doi.org/10.1016/j.jhydrol.2018.10.015.
Kisi, O., 2012. Modeling discharge-suspended sediment relationship using least square support vector machine. J. Hydrol. 456–457, 110–120. https://doi.org/10.1016/j.jhydrol.2012.06.019.
Kisi, O., Alizamir, M., Zounemat-Kermani, M., 2017. Modeling groundwater fluctuations by three different evolutionary neural network techniques using hydroclimatic data. Nat. Hazards 87, 367–381.
Kisi, O., Docheshmeh Gorgij, A., Zounemat-Kermani, M., Mahdavi-Meymand, A., Kim, S., 2019. Drought forecasting using novel heuristic methods in a semi-arid environment. J. Hydrol. 578, 124053. https://doi.org/10.1016/j.jhydrol.2019.124053.
Kisi, O., Yaseen, Z.M., 2019. The potential of hybrid evolutionary fuzzy intelligence model for suspended sediment concentration prediction. CATENA 174, 11–23.
Kitsikoudis, V., Sidiropoulos, E., Hrissanthou, V., 2014. Machine learning utilization for bed load transport in gravel-bed rivers. Water Resour. Manage. 28, 3727–3743. https://doi.org/10.1007/s11269-014-0706-z.
Krause, P., Boyle, D.P., 2005. Advances in geosciences comparison of different efficiency criteria for hydrological model assessment. Adv. Geosci. 5, 89–97. https://doi.org/10.5194/adgeo-5-89-2005.
Kuai, K.Z., Tsai, C.W., 2012. Identification of varying time scales in sediment transport using the Hilbert-Huang Transform method. J. Hydrol. https://doi.org/10.1016/j.jhydrol.2011.12.007.
Kumar, A., Kumar, P., Singh, V.K., 2019. Evaluating different machine learning models for runoff and suspended sediment simulation. Water Resour. Manage. 33, 1217–1231. https://doi.org/10.1007/s11269-018-2178-z.
Lawler, D.M., Petts, G.E., Foster, I.D.L., Harper, S., 2006. Turbidity dynamics during spring storm events in an urban headwater river system: the Upper Tame, West Midlands, UK. Sci. Total Environ. 360, 109–126. https://doi.org/10.1016/j.scitotenv.2005.08.032.
Liu, Q.J., Zhang, H.Y., Gao, K.T., Xu, B., Wu, J.Z., Fang, N.F., 2019. Time-frequency analysis and simulation of the watershed suspended sediment concentration based on the Hilbert-Huang transform (HHT) and artificial neural network (ANN) methods: a case study in the Loess Plateau of China. Catena 179, 107–118. https://doi.org/10.1016/j.catena.2019.03.042.
Lloyd, C.E.M., Freer, J.E., Johnes, P.J., Collins, A.L., 2016. Using hysteresis analysis of high-resolution water quality monitoring data, including uncertainty, to infer controls on nutrient and sediment transfer in catchments. Sci. Total Environ. 543, 388–404. https://doi.org/10.1016/j.scitotenv.2015.11.028.
Lyn, D.A., 1987. Unsteady sediment-transport modeling. J. Hydraul. Eng. 113, 1–15.
Memarian, H., Balasundram, S.K., Tajbakhsh, M., 2013. An expert integrative approach for sediment load simulation in a tropical watershed. J. Integr. Environ. Sci. 10, 161–178.
Moriasi, D.N., Arnold, J.G., Van Liew, M.W., Bingner, R.L., Harmel, R.D., Veith, T.L., Van Liew, M., Bingner, R.L., Harmel, R.D., Veith, T.L., 2007. Model evaluation guidelines for systematic quantification of accuracy in watershed simulations. Trans. ASABE 50, 885–900. https://doi.org/10.13031/2013.23153.
Nayak, P.C., Sudheer, K.P., Rangan, D.M., Ramasastri, K.S., 2004. A neuro-fuzzy computing technique for modeling hydrological time series. J. Hydrol. https://doi.org/10.1016/j.jhydrol.2003.12.010.
Pektas, A.O., Dogan, E., 2015. Prediction of bed load via suspended sediment load using soft computing methods. Geofizika 32, 27–46. https://doi.org/10.15233/gfz.2015.32.2.
Raghavendra, S., Deka, P.C., 2014. Support vector machine applications in the field of hydrology: a review. Appl. Soft Comput. J. 19, 372–386. https://doi.org/10.1016/j.asoc.2014.02.002.
Rahgoshay, M., Feiznia, S., Arian, M., Ali, S., Hashemi, A., 2018. Modeling daily suspended sediment load using improved support vector machine model and genetic algorithm.
Rajaee, T., Nourani, V., Zounemat-Kermani, M., Kisi, O., 2011. River suspended sediment load prediction: application of ANN and wavelet conjunction model. J. Hydrol. Eng. 16, 613–627. https://doi.org/10.1061/(asce)he.1943-5584.0000347.
Riahi-Madvar, H., Seifi, A., 2018. Uncertainty analysis in bed load transport prediction of gravel bed rivers by ANN and ANFIS. Arabian J. Geosci. 11. https://doi.org/10.1007/s12517-018-3968-6.
Roushangar, K., Koosheh, A., 2015. Evaluation of GA-SVR method for modeling bed load transport in gravel-bed rivers. J. Hydrol. 527, 1142–1152.
Roushangar, Kiyoumars, Shahnazi, S., 2019a. Prediction of sediment transport rates in gravel-bed rivers using Gaussian process regression. J. Hydroinf. https://doi.org/10.2166/hydro.2019.077.
Roushangar, K., Shahnazi, S., 2019b. Bed load prediction in gravel-bed rivers using wavelet kernel extreme learning machine and meta-heuristic methods. Int. J. Environ. Sci. Technol. 16, 8197–8208. https://doi.org/10.1007/s13762-019-02287-6.
Sadeghi, S.H.R., Mostafazadeh, R., 2016. Triple diagram models for changeability evaluation of precipitation and flow discharge for suspended sediment load in different time scales. Environ. Earth Sci. https://doi.org/10.1007/s12665-016-5621-6.
Sahraei, S., Alizadeh, M.R., Talebbeydokhti, N., Dehghani, M., 2017. Bed material load estimation in channels using machine learning and meta-heuristic methods. J. Hydroinf. 20, 100–116. https://doi.org/10.2166/hydro.2017.129.
Salih, Sinan Q., Allawi, M.F., Yousif, A.A., Armanuos, A.M., Saggi, M.K., Ali, M., Shahid, S., Al-Ansari, N., Yaseen, Z.M., Chau, K.-W., 2019a. Viability of the advanced adaptive neuro-fuzzy inference system model on reservoir evaporation process simulation: case study of Nasser Lake in Egypt. Eng. Appl. Comput. Fluid Mech. 13, 878–891. https://doi.org/10.1080/19942060.2019.1647879.
Salih, S.Q., Sharafati, A., Khosravi, K., Faris, H., Kisi, O., Tao, H., Ali, M., Yaseen, Z.M., 2019b. River suspended sediment load prediction based on river discharge information: application of newly developed data mining models. Hydrol. Sci. J (accepted for publication).
Sanikhani, H., Kisi, O., Maroufpoor, E., Yaseen, Z.M., 2018. Temperature-based modeling of reference evapotranspiration using several artificial intelligence models: application of different modeling scenarios. Theor. Appl. Climatol. 1–14. https://doi.org/10.1007/s00704-018-2390-z.
Sharghi, E., Nourani, V., Najafi, H., Gokcekus, H., 2019a. Conjunction of a newly proposed emotional ANN (EANN) and wavelet transform for suspended sediment load modeling. Water Supply 19, 1726–1734. https://doi.org/10.2166/ws.2019.044.
Sharghi, E., Nourani, V., Najafi, H., Soleimani, S., 2019b. Wavelet-exponential smoothing: a new hybrid method for suspended sediment load modeling. Environ. Processes 6, 191–218. https://doi.org/10.1007/s40710-019-00363-0.
Šiljić Tomić, A., Antanasijević, D., Ristić, M., Perić-Grujić, A., Pocajt, V., 2018. A linear and non-linear polynomial neural network modeling of dissolved oxygen content in surface water: inter- and extrapolation performance with inputs' significance analysis. Sci. Total Environ. 610–611, 1038–1046. https://doi.org/10.1016/j.scitotenv.2017.08.192.
Sreedhara, B.M., Rao, M., Mandal, S., 2018. Application of an evolutionary technique (PSO–SVM) and ANFIS in clear-water scour depth prediction around bridge piers. Neural Comput. Appl. https://doi.org/10.1007/s00521-018-3570-6.
Talei, A., Chua, L.H.C., Quek, C., 2010. A novel application of a neuro-fuzzy computational technique in event-based rainfall–runoff modeling. Expert Syst. Appl. 37 (12), 7456–7468.
Takagi, T., Sugeno, M., 1985. Fuzzy identification of systems and its applications to modeling and control. IEEE Trans. Syst. Man Cybernet. SMC-15, 116–132. https://doi.org/10.1109/TSMC.1985.6313399.
Tao, H., Keshtegar, B., Yaseen, Z.M., 2019. The Feasibility of Integrative Radial Basis M5Tree Predictive Model for River Suspended Sediment Load Simulation. Water Resour. Manage. 33, 4471–4490. https://doi.org/10.1007/s11269-019-02378-6.
Taylor, K.E., 2001. Summarizing multiple aspects of model performance in a single diagram. J. Geophys. Res.: Atmos. 106, 7183–7192. https://doi.org/10.1029/2000JD900719.
Torabi, H., Dehghani, R., 2018. Comparison and evaluation of intelligent models for river suspended sediment estimation (case study: Kakareza River, Iran). Environ. Resour. Res. 6, 139–148.

Vapnik, V.N., 1998. In: Statistical Learning Theory. John Wiley & Sons. https://doi.org/10.2307/1271368.

Willmott, C.J., Matsuura, K., 2005. Advantages of the mean absolute error (MAE) over the root mean square error (RMSE) in assessing average model performance. Clim. Res. 30, 79–82. https://doi.org/10.3354/cr030079.

Yadav, A., Chatterjee, S., Equeenuddin, S.M., 2018. Suspended sediment yield estimation using genetic algorithm-based artificial intelligence models: case study of Mahanadi River, India. Hydrol. Sci. J. 63, 1162–1182. https://doi.org/10.1080/02626667.2018.1483581.

Yaseen, Z.M., Ehteram, M., Hossain, M.S., Fai, C.M., Koting, S.B., Mohd, N.S., Jaafar, W.Z.B., Afan, H.A., Hin, L.S., Zaini, N., Ahmed, A.N., El-Shafie, A., 2019. A novel hybrid evolutionary data-intelligence algorithm for irrigation and power production management: application to multi-purpose reservoir systems. Sustainability (Switzerland). https://doi.org/10.3390/su11071953.

Yaseen, Z.M., Jaafar, O., Deo, R.C., Kisi, O., Adamowski, J., Quilty, J., El-Shafie, A., 2016. Stream-flow forecasting using extreme learning machines: a case study in a semi-arid region in Iraq. J. Hydrol. 542, 603–614. https://doi.org/10.1016/j.jhydrol.2016.09.035.

Yilmaz, B., Aras, E., Nacar, S., Kankal, M., 2018. Estimating suspended sediment load with multivariate adaptive regression spline, teaching-learning based optimization, and artificial bee colony models. Sci. Total Environ. 639, 826–840. https://doi.org/10.1016/j.scitotenv.2018.05.153.

Zounemat-Kermani, M., 2017. Assessment of several nonlinear methods in forecasting suspended sediment concentration in streams. Hydrol. Res. 48, 1240–1252. https://doi.org/10.2166/nh.2016.219.

Zounemat-Kermani, M., Kişi, Ö., Adamowski, J., Ramezani-Charmahineh, A., 2016. Evaluation of data driven models for river suspended sediment concentration modeling. J. Hydrol. 535, 457–472. https://doi.org/10.1016/j.jhydrol.2016.02.012.

Zounemat-Kermani, M., Kisi, O., Piri, J., Mahdavi-Meymand, A., 2019. Assessment of artificial intelligence-based models and metaheuristic algorithms in modeling evaporation. J. Hydrol. Eng. 24, 4019033. https://doi.org/10.1061/(asce)he.1943-5584.0001835.